

HyNECC: Hypersonic NonEquilibrium Comparison Cases SU2-NEMO results for Phase 1: N₂/N, O₂/O and 5-species air in 0D adiabatic bath

Catarina Garbacz^{*}, Fábio Morgado-Pereira[†] and Marco Fossati[‡]
Aerospace Centre, University of Strathclyde, Glasgow, G1 1XJ, United Kingdom

Michele Capriati[§] and Thierry Magin[¶]
von Karman Institute for Fluid Dynamics, Rhode-Saint-Genese, 1640, Belgium

I. Introduction

THE open-source SU2-NEMO (NonEquilibrium MOdels) software suite [1] written in C++ and Python is the basis for this study. It is built specifically to simulate chemically-reactive and nonequilibrium flows with state-of-the-art numerical methods. The numerical model adopted is based on classical literature on the subject. A finite-volume edge-based formulation is used with the AUSM scheme [2] together with MUSCL and standard limiting procedures. A time-stepping approach with a second-order backwards-difference discretization of the time derivative terms is adopted to address time evolution. Thermochemistry models are implemented by linking SU2-NEMO to the Mutation++ library [3] (Multicomponent Thermodynamic And Transport properties for IONized gases in C++), that provides efficient algorithms for the computation of thermodynamic, transport (viscosity, thermal conductivity and diffusion) and chemical kinetic gas properties. The library has been designed for robustness over a wide range of temperatures and its accuracy in dealing with multi-temperature models, with the following constraints in mind: 1) high fidelity of the physical models, ensuring that the laws of thermodynamics are satisfied and that results are validated against existing experimental data, 2) low computational cost, 3) a modern, object-oriented, extensible framework, and 4) detailed in-source and user's guide documentation in order to facilitate model improvement and collaboration.

II. Theoretical models

The system of governing equations used in the simulations of the 0D adiabatic bath is given by

$$\frac{d\mathbf{U}}{dt} = \mathbf{Q}(\mathbf{U}). \quad (1)$$

The two-temperature model by Park [4] is used, where the translational energy mode is assumed to be at equilibrium

^{*}PhD student, Dept. Mechanical and Aerospace Engineering, 75 Montrose street, G1 1XJ Glasgow, and AIAA Member.

[†]PhD student, Dept. Mechanical and Aerospace Engineering, 75 Montrose street, G1 1XJ Glasgow, and AIAA Member.

[‡]Associate Professor, Dept. Mechanical and Aerospace Engineering, 75 Montrose street, G1 1XJ Glasgow, and AIAA Member.

[§]PhD student, Department of Aeronautics and Aerospace, AIAA Member.

[¶]Associate Professor, Department of Aeronautics and Aerospace, AIAA Member.

with the rotational one, and the vibrational energy mode is assumed to be at equilibrium with the electronic one. The vectors of conservative variables and source terms are defined as

$$\mathbf{U} = \begin{pmatrix} \rho_1 \\ \vdots \\ \rho_{n_s} \\ \rho e \\ \rho e^{v-e} \end{pmatrix}, \quad \mathbf{Q} = \begin{pmatrix} \dot{\omega}_1 \\ \vdots \\ \dot{\omega}_{n_s} \\ 0 \\ \dot{\Omega} \end{pmatrix}, \quad (2)$$

and ρ is the density of the mixture, ρ_s is the density of species s , e and e^{v-e} are, respectively, the internal energy per unit mass and the vibrational energy per unit mass for the mixture, index s denotes the s^{th} chemical species and n_s is the total number of species.

Calculating the nonequilibrium thermodynamic state and source terms is necessary to close the system of governing equations. The equations presented below describe the implementation of the two-temperature model for a mixture composed of neutral species, provided by the Mutation++ library [3]. Each individual species s is assumed to behave as an ideal gas. Hence, the total pressure of the mixture p is defined by Dalton's Law as the summation of the partial pressures associated with each species p_s , determined by the ideal gas law,

$$p = \sum_{s=1}^{n_s} p_s = \sum_{s=1}^{n_s} \rho_s \frac{R_u}{M_s} T_{\text{tr}}, \quad (3)$$

where R_u is the universal gas constant, M_s is the molar mass of species s and T_{tr} is the trans-rotational temperature. The internal specific energy of the flow e is given as the weighted sum of the species internal energies:

$$e = \sum_{s=1}^{n_s} c_s e_s, \quad (4)$$

where c_s is the mass fraction of species s and e_s is the specific internal energy of the species, given by the sum of the energy of formation and the contribution of each internal mode,

$$e_s = e_s^{\text{t}}(T_{\text{tr}}) + e_s^{\text{r}}(T_{\text{tr}}) + e_s^{\text{v}}(T_{\text{ve}}) + e_s^{\text{e}}(T_{\text{ve}}) + e_s^0. \quad (5)$$

The internal mode energies are defined on the basis of the Rigid-Rotor/Harmonic Oscillator model (RRHO) as:

$$e_s^t(T_{tr}) = \frac{3}{2} \frac{R_u}{M_s} T_{tr}, \quad (6)$$

$$e_s^r(T_{tr}) = \begin{cases} \frac{R_u}{M_s} T_{tr}, & \text{for molecules,} \\ 0, & \text{for atoms,} \end{cases} \quad (7)$$

$$e_s^v(T_{ve}) = \begin{cases} \frac{R_u}{M_s} \frac{\theta_s^v}{\exp(\theta_s^v/T_{ve}) - 1}, & \text{for molecules,} \\ 0, & \text{for atoms,} \end{cases} \quad (8)$$

$$e_s^e(T_{ve}) = \frac{R_u}{M_s} \frac{\sum_i g_{i,s} \theta_{i,s}^e \exp(-\theta_{i,s}^e/T_{ve})}{\sum_i g_{i,s} \exp(-\theta_{i,s}^e/T_{ve})}, \quad (9)$$

where θ_s^v is the characteristic vibrational temperature of species s , $g_{i,s}$ and $\theta_{i,s}^e$ are the degeneracy and characteristic electronic temperature, respectively, at energy level i for species s . The formation energy e_s^0 is referenced at the standard state conditions of 298.15 K and 1 atm. The characteristic vibrational temperatures are $\theta_{N_2}^v = 3408.464$ K and $\theta_{O_2}^v = 2276.979$ K. The characteristic electronic temperatures $\theta_{i,s}^e$ and the degeneracy of each electronic level $g_{i,s}$ are given in Tables 2-6.

The change in vibrational energy of the mixture is accounted for in the source term $\dot{\Omega}$, that is defined as the sum of the vibrational-to-translational energy transfer and energy exchanges due to chemical activity,

$$\dot{\Omega} = \sum_{s=1}^{n_s} \dot{\Omega}_s^{t-r:v-e} + \dot{\Omega}_s^{c:v} + \dot{\Omega}_s^{c:e}. \quad (10)$$

A. Internal energy transfer

The term $\dot{\Omega}_s^{t-r:v-e}$ in equation 10 concerns the rate of energy exchange between the translational and vibrational energy modes, following the Landau-Teller model [5]

$$\dot{\Omega}_s^{t-r:v-e} = \rho_s \frac{e_s^v(T) - e_s^v(T_v)}{\tau_s^{v-T}}. \quad (11)$$

The vibrational relaxation time of each species, τ_s^{v-T} , is given by the Millikan and White empirical formula [6] and the Park correction [7],

$$\tau_s^{v-T} = \tau_s^{MW} + \tau_s^P, \quad (12)$$

where the Millikan and White relaxation time of species s depends on the vibrational relaxation times of the interactions with collision partners r and the corresponding molar fractions X_r , as follows

$$\tau_s^{\text{MW}} = \left(\sum_{r=1}^{n_s} \frac{X_r}{\tau_{s-r}^{\text{MW}}} \right)^{-1}, \quad (13)$$

$$\tau_{s-r}^{\text{MW}} = \exp \left(A_{s,r} \left(T^{-\frac{1}{3}} - B_{s,r} \right) - 18.42 \right) \left(\frac{P}{101325} \right)^{-1} [s]. \quad (14)$$

The parameters $A_{s,r}$ and $B_{s,r}$ used in the Millikan and White model are given in Table 1 of the appendix. The Park correction is given by

$$\tau_s^{\text{P}} = \left(N_s \sigma_s \sqrt{\frac{8R_u T_{\text{tr}}}{\pi M_s}} \right)^{-1}, \quad (15)$$

where X_r is the molar fraction, N_s is the number density and σ_s is an effective cross-section for vibrational relaxation, given by

$$\sigma_s = \begin{cases} \sigma'_s \left(\frac{50,000}{20,000} \right)^2, & \text{for } T > 20,000 \\ \sigma'_s \left(\frac{50,000}{T_{\text{tr}}} \right)^2, & \text{otherwise,} \end{cases} \quad (16)$$

with $\sigma'_s = 3 \times 10^{-17} \text{ cm}^2$ for N_2 , O_2 and NO .

B. Multi-temperature reaction rates

The chemical source term $\dot{\omega}_s$ that accounts for production/destruction of species mass is given by

$$\dot{\omega}_s = M_s \sum_{r=1}^{n_r} (\nu''_{s,r} - \nu'_{s,r}) \left[k_{\text{f},r} \prod_{j=1}^{n_s} \hat{\rho}_j^{\nu'_{j,r}} - k_{\text{b},r} \prod_{j=1}^{n_s} \hat{\rho}_j^{\nu''_{j,r}} \right], \quad (17)$$

where n_r and n_s are, respectively, the number of reactions and the number of species, ν'_s is the forward reaction stoichiometry coefficient, ν''_s is the backward reaction stoichiometry coefficient, $\hat{\rho}_j$ is the molar density, $k_{\text{f},r}$ is the forward reaction rate and $k_{\text{b},r}$ is the backward reaction rate. The forward reaction rate for each reaction r is defined according to the modified Arrhenius equation

$$k_{\text{f},r} = A_r T_c^{N_r} \exp \left(-\frac{\theta_r}{T_c} \right), \quad (18)$$

where the coefficients A_r , θ_r and N_r are obtained from experimental data and are, respectively, the reaction rate constant, the activation temperature and an exponent. The reactions mechanisms and Arrhenius formula coefficients used in this study are given in section B of the appendix. T_c is the controlling temperature determined by Park's two-temperature

model [4]:

- Dissociation reactions $AB + M \rightleftharpoons A + B + M$

$T_c = \sqrt{T_{tr}T_{ve}}$ for the forward rate; $T_c = T_{tr}$ for the backward rate;

- Exchange reactions $AB + C \rightleftharpoons A + BC$

$T_c = T_{tr}$.

C. Energy removed or added per reaction

The change in vibrational-electronic energy of the mixture due to the production/destruction of species is accounted for in the terms $\dot{\Omega}_s^{c:v}$ and $\dot{\Omega}_s^{c:e}$, given by

$$\dot{\Omega}_s^{c:v} = c_1 \dot{\omega}_s e_s^v, \quad \dot{\Omega}_s^{c:e} = \dot{\omega}_s e_s^e. \quad (19)$$

Both preferential and non-preferential dissociation models are used in this study to account for the coupling between vibrational energy modes and finite-rate chemistry. For the non-preferential dissociation model, which assumes that molecules are destroyed or created at the average vibrational energy of the cell, $c_1 = 1$. For the preferential dissociation model, it is considered that molecules dissociate more easily when vibrationally more excited and therefore must "ladder climb" from lower to higher vibrational states to be dissociated - in this case $c_1 = 0.3$.

D. Reverse reactions and $K_{eq}(T)$

The backward reaction rates $k_{b,r}$ are determined from the equilibrium reaction rates

$$k_{b,r} = k_{f,r} / K_{eq,r} \quad (20)$$

for every reaction r . The equilibrium reaction rates $K_{eq,r}$ are determined as a function of the Gibbs free energy as follows

$$K_{eq,r} = \left(\frac{p^0}{R_u T} \right)^{\Delta \nu_r} \exp \left(- \frac{\Delta G_r^0}{R_u T} \right), \quad (21)$$

$$\Delta \nu_r = \sum_s (\nu''_{s,r} - \nu'_{s,r}), \quad (22)$$

$$\Delta G_r^0 = \sum_s (\nu''_{s,r} - \nu'_{s,r}) G_s^0. \quad (23)$$

III. Contributed results

A. TC1A.1 - N₂/N

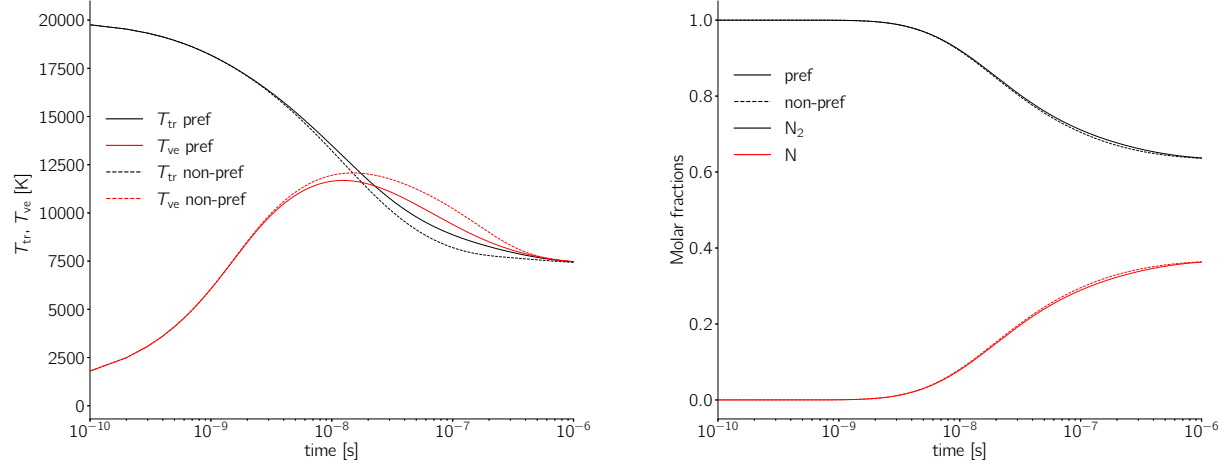


Fig. 1 Adiabatic 0D bath simulation for an N₂-N mixture: temperatures (left) and species molar fractions (right).

B. TC1A.2 - O₂/O

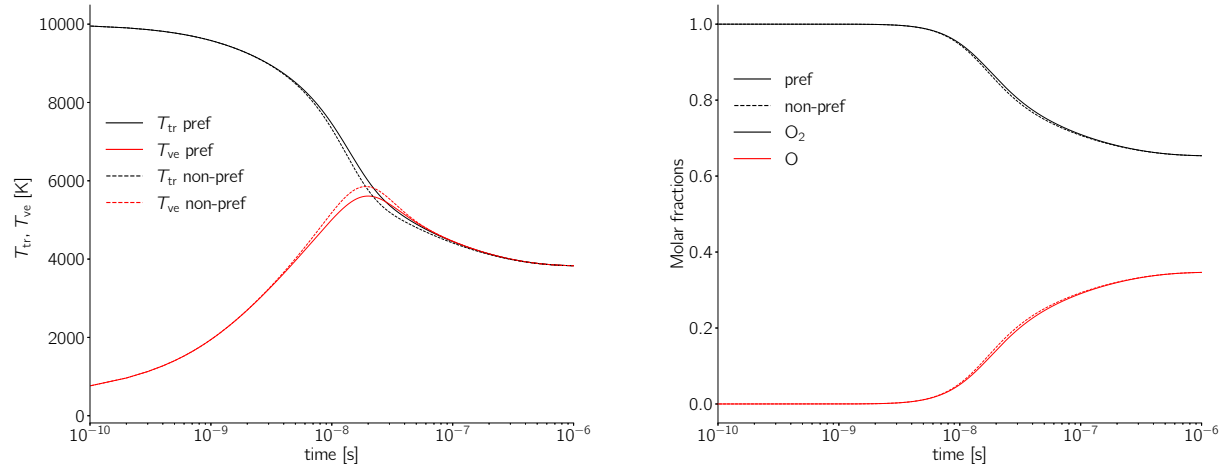


Fig. 2 Adiabatic 0D bath simulation for an O₂-O mixture: temperatures (left) and species molar fractions (right).

C. TC1A.3 - Air (79% N₂, 21%O₂)

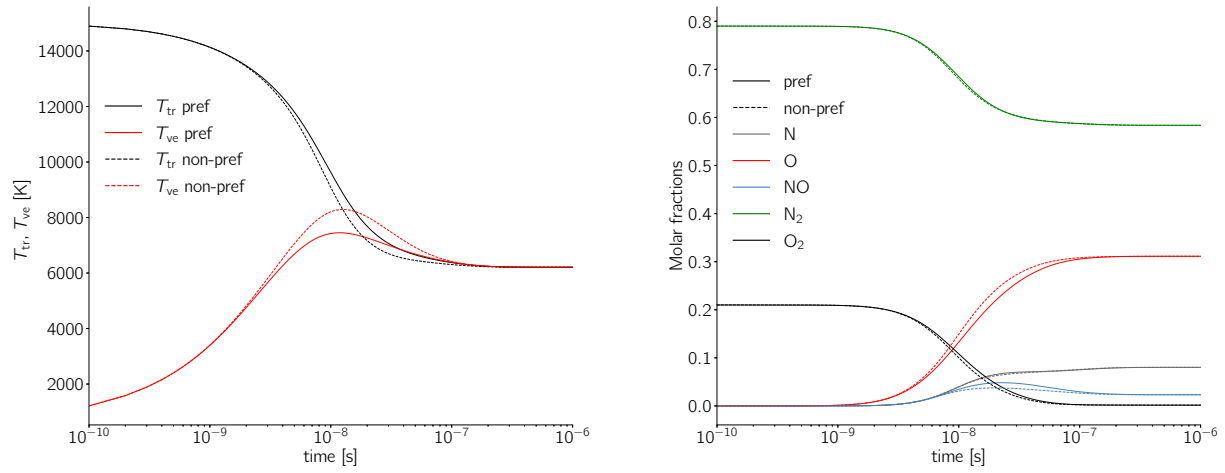


Fig. 3 Adiabatic 0D bath simulation for an air 5-species mixture: temperatures (left) and species molar fractions (right).

References

- [1] Economou, T. D., Palacios, F., Copeland, S. R., Lukaczyk, T. W., and Alonso, J. J., "SU2: An Open-Source Suite for Multiphysics Simulation and Design," *AIAA Journal*, Vol. 54, No. 3, 2016, pp. 828–846. <https://doi.org/10.2514/1.J053813>.
- [2] Liou, M.-S., and Steffen, C. J., "A New Flux Splitting Scheme," *Journal of Computational Physics*, Vol. 107, No. 1, 1993, pp. 23–39.
- [3] Scoggins, J. B., Leroy, V., Bellas-Chatzigeorgis, G., Dias, B., and Magin, T. E., "Mutation++: Multicomponent Thermodynamic And Transport properties for IONized gases in C++," *SoftwareX*, Vol. 12, 2020, p. 100575. <https://doi.org/https://doi.org/10.1016/j.softx.2020.100575>.
- [4] Park, C., "Assessment of two-temperature kinetic model for ionizing air," *Journal of Thermophysics and Heat Transfer*, Vol. 3, No. 3, 1989, pp. 233–244. <https://doi.org/10.2514/3.28771>.
- [5] Landau, L., and Teller, E., "Systematics of Vibrational Relaxation," *Physik Zeitschrift der Sowjetunion*, Vol. 10, 1936, pp. 34–38.
- [6] Millikan, R. C., and White, D. R., "Systematics of Vibrational Relaxation," *The Journal of Chemical Physics*, Vol. 39, No. 12, 1963, pp. 3209–3213. <https://doi.org/10.1063/1.1734182>.
- [7] Park, C., "Review of chemical-kinetic problems of future NASA missions. I - Earth entries," *Journal of Thermophysics and Heat Transfer*, Vol. 7, No. 3, 1993, pp. 385–398. <https://doi.org/10.2514/3.431>.

Appendices

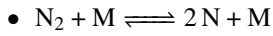
A. Internal energy transfer

Table 1 Millikan and White model coefficients [7]

Species s	Partner Species r	$A_{s,r}$	$B_{s,r}$
N_2	N	180.0	0.0262
	O	72.40	0.0150
	N_2	221.0	0.0290
	O_2	229.0	0.0295
	NO	225.0	0.0293
O_2	N	72.40	0.0150
	O	47.70	0.0590
	N_2	134.0	0.0295
	O_2	138.0	0.0300
	NO	136.0	0.0298
NO	N	49.50	0.0420
	O	49.50	0.0420
	N_2	49.50	0.0420
	O_2	49.50	0.0420
	NO	49.50	0.0420

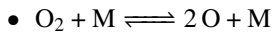
B. Reaction mechanisms and Arrhenius coefficients [7]

1. TCIA.1



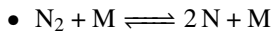
$$A_r = 3 \times 10^{22} \text{ cm}^3 \text{ mol}^{-1} \text{ s}^{-1}; N_r = -1.6; \theta_r = 113,200 \text{ K};$$

2. TCIA.2

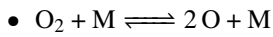


$$A_r = 1 \times 10^{22} \text{ cm}^3 \text{ mol}^{-1} \text{ s}^{-1}; N_r = -1.5; \theta_r = 59,360 \text{ K};$$

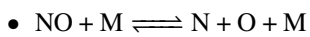
3. TCIA.3



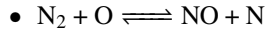
$$A_r = 3 \times 10^{22} \text{ cm}^3 \text{ mol}^{-1} \text{ s}^{-1}; N_r = -1.6; \theta_r = 113,200 \text{ K};$$



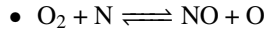
$$A_r = 1 \times 10^{22} \text{ cm}^3 \text{ mol}^{-1} \text{ s}^{-1}; N_r = -1.5; \theta_r = 59,360 \text{ K};$$



$$A_r = 5 \times 10^{15} \text{ cm}^3 \text{ mol}^{-1} \text{ s}^{-1}; N_r = 0.0; \theta_r = 75,500 \text{ K};$$



$$A_r = 5.69 \times 10^{12} \text{ cm}^3 \text{ mol}^{-1} \text{ s}^{-1}; N_r = 0.42; \theta_r = 42,938 \text{ K};$$



$$A_r = 2.49 \times 10^9 \text{ cm}^3 \text{ mol}^{-1} \text{ s}^{-1}; N_r = 1.18; \theta_r = 4,005.5 \text{ K};$$

C. Electronic levels: degeneracy and characteristic temperatures

Table 2 N_2 .

i	Degeneracy	$\theta_{i,s}$ [K]
0	1	0.0
1	3	72227.8
2	6	85774.1
3	6	86045.8
4	3	95346.2
5	1	98051.3
6	2	99677.5
7	2	103726.8

Table 3 O_2 .

i	Degeneracy	$\theta_{i,s}$ [K]
0	3	0.0
1	2	11390.9
2	1	18983.8
3	1	47557.2
4	6	49909.8
5	3	50920.1
6	3	71635.9

Table 4 NO .

i	Degeneracy	$\theta_{i,s}$ [K]
0	4	0.0
1	8	54670.6

Table 5 N.

i	Degeneracy	$\theta_{i,s}$ [K]
0	4	0.0
1	10	27663.3
2	6	41495.0
3	12	119891.2
4	6	124011.6
5	12	126795.5
6	2	134640.7
7	20	136450.6
8	12	137414.6
9	4	139201.4
10	10	139316.5
11	6	140697.7
12	10	143389.5
13	12	149180.2
14	6	149911.1
15	6	150526.9
16	28	150665.0
17	26	150850.6
18	20	151083.6
19	10	151257.7
20	2	153195.7
21	20	153694.9
22	12	153961.0
23	10	154263.2
24	4	154588.3
25	6	154831.5
26	12	158091.5
27	6	158370.7
28	90	158730.3
29	126	158892.9
30	24	159172.0
31	2	159786.3
32	38	160041.0
33	4	160413.6
34	10	160970.4
35	6	161584.7
36	18	162095.5
37	60	162315.6
38	126	162443.6
39	32	163082.4
40	18	164184.4
41	90	164312.5
42	180	164358.5
43	20	164798.8
44	108	165472.1
45	18	166122.4

Table 6 O.

i	Degeneracy	$\theta_{i,s}$ [K]
1	9	0.0
2	5	22859.5
3	1	48619.4
4	5	106130.0
5	3	110480.7
6	15	124625.9
7	9	127527.8
8	5	137367.1
9	3	138434.6
10	25	140292.0
11	15	140407.0
12	15	142729.1
13	9	143540.5
14	15	145629.5
15	5	147022.2
16	3	147485.5
17	5	147833.6
18	25	148066.7
19	15	148181.8
20	56	148298.3
21	15	149226.3
22	9	149574.4
23	5	151198.7
24	3	151431.8
25	40	151780.0
26	56	151860.5
27	15	152359.8
28	9	152476.3
29	5	153404.3
30	3	153520.8
31	168	153752.4
32	5	154680.4
33	3	154796.9
34	96	154948.0
35	8	11761.4
36	40	155701.9
37	8	156178.1
38	40	156235.6
39	3	156572.3
40	40	156606.8